



Preparation and Characterization of Cellulose Acetate /Ag-TiO₂ Nanocomposite Films for Food Packaging Application

Journal:	<i>Polymers and Polymer Composites</i>
Manuscript ID	PPC-22-0016
Manuscript Type:	Original Research Article
Date Submitted by the Author:	23-Jan-2022
Complete List of Authors:	Ali, Hajer; University of Technology, Department of Applied Science-material Science brach Hammed, Nahida; University of Technology, Department of Applied Science-material Science branch
Keywords:	Antibacterial activity, Biodegradable, Biopolymer, Contact angle, Mechanical properties
Abstract:	Nanocomposite film of Cellulose Acetate/Ag-TiO ₂ were synthesized by cast method at different weight ratios of Ag nanoparticle (1.5, 2, 2.5) wt% and a constant weight ratio of 2 wt%TiO ₂ . The mechanical properties (Tensile strength and elongation) were improved at fixed level of CA+ 2%TiO ₂ +1.5% Ag loading, beyond that level of loading, it decreased. The tensile strength was decreased due to some degrees of agglomeration of filler particles above a critical content. FTIR were conducted chemical composition of as-prepared composite films. The wettability of the films was also determined by Sessile drop method, an increase in contact angle was also observed by the addition of Ag content from 70.2° to 76.4° compared to pure CA that indicated a value of 61.3°. Antibacterial activity against Escherichia coli and Staphylococcus aureus were enhanced after incorporation of Ag-TiO ₂ compared with pure CA. The enhanced wettability and antibacterial activity of the prepared films suggest that they could be used for Packaging applications.

SCHOLARONE™
Manuscripts

1
2
3
4 **Preparation and Characterization of Cellulose Acetate**
5
6 **/Ag-TiO₂ Nanocomposite Films for Food Packaging**
7
8 **Application**
9

10 Hajer A Ali^{2,1*} and Nahida J. Hammed^{1**}

11 ¹Materials science – Department of Applied sciences, University of Technology -Iraq

12 ²Ministry of Agriculture/ Mesopotamian state company of seeds, Baghdad, Iraq

13 *as.18.47@grad.uotechnology.edu.iq

14 **nahidajoumaa61@yahoo.com

15
16
17
18
19
20
21
22
23
24
25
26
27
28
29
30
31
32
33
34
35
36
37
38
39
40
41
42
43
44
45
46
47
48
49
50
51
52
53
54
55
56
57
58
59
60

For Peer Review

Preparation and Characterization of Cellulose Acetate /Ag-TiO₂ Nanocomposite Films for Food Packaging Application

Abstract

Nanocomposite film of Cellulose Acetate/Ag-TiO₂ were synthesized by cast method at different weight ratios of Ag nanoparticle (1.5, 2, 2.5) wt% and a constant weight ratio of 2 wt%TiO₂. The mechanical properties (Tensile strength and elongation) were improved at fixed level of CA+ 2%TiO₂ +1.5% Ag loading, beyond that level of loading, it decreased. The tensile strength was decreased due to some degrees of agglomeration of filler particles above a critical content. FTIR were conducted chemical composition of as-prepared composite films. The wettability of the films was also determined by Sessile drop method, an increase in contact angle was also observed by the addition of Ag content from 70.2° to 76.4° compared to pure CA that indicated a value of 61.3°. Antibacterial activity against Escherichia coli and Staphylococcus aureus were enhanced after incorporation of Ag-TiO₂ compared with pure CA. The enhanced wettability and antibacterial activity of the prepared films suggest that they could be used for Packaging applications.

Keywords: Antibacterial activity, biodegradable, biopolymer, Contact angle, Mechanical properties.

1. Introduction

Packaging technology provides endless opportunities for food preservation, and biopolymer-based films have been frequently employed in Packaging because of their edible, renewable, and biodegradable properties [1-5]. Due to benefits such as good appearance, biodegradability, excellent durability,

1
2
3 and nontoxicity, cellulose acetate manufactured from naturally occurring
4 cellulose materials such as wood, cotton, and rice husk is a green product
5 nominated for producing food packaging films [6-8]. It's used in a variety of
6 applications, including filters, drug delivery, and medical implants [9-
7 12]. Nanoparticles such as Ag, Au, Zn, ZnO, Titanium dioxide, and Cerium
8 dioxide have been employed to make composite functional films to extend
9 the functionality of packaging [13–15]. TiO₂ nanoparticles have gained a lot
10 of interest because of their stable nature, ability to inhibit bacterial growth
11 and prevent further formation of cell structures, environmental friendliness,
12 low cost and good photocatalytic performance [16,17]. The US Food and
13 Drug Administration (USFDA) has fully cleared the use of TiO₂
14 nanoparticles as food additives and food contact compounds after a safety
15 assessment [18]. The incorporation of nanoparticles such as Au, Ag into
16 TiO₂ nanostructures has been stated to improve visible light absorption due
17 to high surface plasmon resonance excitation [19,20]. In comparison to Au
18 nanoparticles and pure TiO₂ nanoparticles, SPR excitation can expedite the
19 interfacial charge transfer between Au and TiO₂ nanoparticles, resulting in
20 increased photocatalytic activity. [21–23]. Furthermore, Au-incorporated
21 TiO₂ nanocomposites have been shown to have low toxicity [24]. Cellulose
22 acetate films with Ag-TiO₂ nanocomposite integrated are made and applied
23 to packaging in this study. The Ag-TiO₂ nanocomposite-incorporated films'
24 physical and chemical properties, as well as antibacterial activity and contact
25 angle, are all measured.

2. Material and methods

2.1 Materials

CA (CDH India, acetyl content 29-45%; Maximum limit of impurities;
0.1%; free acid (as acetic acid); 5.0%; loss on drying at 105°C sulphated ash;
0.1%)) and Acetone AR/ACS (2-Propanone, Dimethylketone) (M.W.:58.08)

1
2
3 from CDH India. Titanium oxide nanoparticles/nanopowder (TiO_2 , Rutile,
4 99.5%), particle size (20-40) nm was purchased from Skyspring,USA.
5
6 Hongwu international group ltd-china supplied Ag nanoparticle with particle
7 sizes ranging from 40 to 80 nm.
8
9
10

11 12 **2. 2 Methodology**

13 14 **2.2.1 Preparation of primary polymer solutions**

15
16 The CA primary solution was prepared by the dissolution of 7 g of CA in
17 100 ml of acetone using the casting method. The solution was then stirred
18 for 8 h using a magnetic stirrer and then cast in a glass petri dish, and then a
19 final film was obtained after 48 h.
20
21
22
23
24
25

26 27 **2.2.2 Preparation of Ag/ TiO_2 /CA composite polymer solution**

28
29 Ag and TiO_2 nanoparticles Solution were added to CA Powder at different
30 weight ratio of Ag nanoparticle (1.5, 2, 2.5 wt%) and a constant weight ratio
31 of 2% TiO_2 of composite film. The mixture was stirred until get the
32 homogeneous solutions; Then the solution was casted in a glass Petri dish;
33 and left to dry for 48 hrs. the preparation process was shown in Figure.1.
34
35
36
37
38
39
40
41

42 **[insert Figure 1.]**

43
44 Fig. 1. Schematic diagram of the preparation process for the films.
45
46
47

48 **3. Characterization**

49
50 The morphology of the powder was examined with FESEM Zeiss Sigma
51 300-HV Germany. The mechanical characteristics of the cellulose acetate
52 and the composites thick films were measured by tensile tests using Laryee
53 Universal Testing Machine (UTM) UE3450 from Laryee Technology Co.,
54 Ltd. China. The films were cut to 120 mm \times 10 mm, and the thickness were
55
56
57
58
59
60

1
2
3 measured by a digital micrometer with $\pm 1 \mu\text{m}$ accuracy. All the tests were
4 performed at room temperature (around 27°C) and a crosshead speed of 5
5 mm/min. was used during the measurements of the cellulose based films,
6 and a stress-strain curve was recorded. Young's modulus, elongation at
7 break point and ultimate tensile strength were determined by a well-known
8 standard procedure.
9
10
11
12
13
14
15

16
17 Fourier transformed infrared FTIR spectra were obtained by SHIMADZU-
18 8400S FTIR spectrometer, Japan. The spectra were obtained in the
19 wavenumber range of $400\text{-}4000 \text{ cm}^{-1}$, 4 cm^{-1} resolution. The samples were
20 prepared as tablets by mixing with KBr powder.
21
22
23
24
25

26 The optical system used to measure contact angle was from Holmarc Opto-
27 Mechatronics P Ltd. India, with automated dispenser and software for static
28 and dynamic contact angle measurement. A drop of water is placed on the
29 film surface and it will spread on the surface based on the interactions
30 between the solid surface and the water. Water contact angle will be
31 measured to give an indication of the wettability of the surface.
32
33
34
35
36
37
38

39 The antibacterial activity of the CA and CA/TiO₂/Ag was tested against
40 human pathogens Escherichia coli and Staphylococcus aureus using the
41 following protocol. The bacteria were captured from their stock cultures
42 using a sterile wire loop. To assess how CA and CA/TiO₂/Ag have an
43 impact on the bacteria's growth curve, the bacterial strains were grown at
44 37°C on M-H agar plates with immunization of 50 mL of nutrient broth.
45 The bacterial growth grew up until the nutritional broth attained an optical
46 density (OD) of 0.1 at 600 nm, which corresponds to a bacterial
47 concentration of 10^8 CFU/mL . The bacterial cultures (1 mL) were then
48 added to the nutritional broth along with CA and CA/TiO₂/Ag, and
49 incubated at 37°C for 12 hours with slight agitation. The OD was measured
50
51
52
53
54
55
56
57
58
59
60

with a spectrophotometer to determine bacterial growth. An unpaired t-test was used to statistically assess the obtained data. The results were provided as the mean \pm SD of triplicate measurements.

Results and discussion

4.1 SEM analysis

SEM micrographs of TiO₂, Ag powders are shown in fig 2 a to b.

[insert Figure 2.]

Fig.2. SEM images of (a) TiO₂ nanoparticle, (b) Ag nanoparticle.

As clearly shown TiO₂, Ag nano powder have very fine particle size with narrow distribution of about 20-40nm and 40-80nm respectively. Fine particles have a high degree of agglomeration due to their high surface area, so a more sophisticated dispersion technique will be required to prevent agglomeration and to achieve a higher homogeneity of the particle distribution within the CA matrix.

4.2 Tensile test

The stress-strain curves for Ag-TiO₂ /CA composite films at different weight ratios of Ag nanoparticle (1.5, 2, 2.5) wt% and a constant weight ratio of 2 wt% TiO₂ are shown in Fig. 3. The good distribution of inorganic fillers in the (CA) polymer matrix was responsible for the improvement in mechanical properties by up to 1.5 wt% Ag and 2%TiO₂ [25-27]. The mechanical properties of polymer systems depend on the intermolecular force chain, stiffness, and molecular symmetry of polymer systems [28]. Polymers with a high degree of crystallinity, crosslinking, or rigid chains have a high strength or limited extendibility, resulting in a high yield modulus, a high stress at peak value, and a low elongation value. CA is a

1
2
3 rigid, strong material that exhibits a dipole-dipole attraction due to
4 electrostatic interactions between the ester atoms of one chain and the
5 hydroxyl atoms of another. The interaction of dipole-dipole attraction, which
6 reaches its maximum magnitude, was associated with the improvement in
7 mechanical characteristics. The increase in strength can be attributed to an
8 increase in the filler's capacity to adhere to the matrix, which resulted in less
9 sliding between the composite layers when stress was applied to the
10 composites [29,30].
11
12
13
14
15
16
17
18
19

20
21 **[insert Figure 3.]**
22

23 Fig.3. stress-strain curve of Ag/TiO₂ with Cellulose acetate.
24
25

26 The tensile strength is reduced due to some degrees of agglomeration of
27 filler particles above the critical content and an increase in inhomogeneity
28 [26, 27]. The lack of interfacial adhesion between the polymer and the fillers
29 was responsible for the decrease in tensile strength [30].
30
31
32
33

34 At fixed level of 1.5%Ag- 2% TiO₂/CA loading; both tensile strength and
35 elongation were improved as shown in Fig. 4, beyond that level of loading
36 the values of tensile strength and elongation decreased.
37
38
39
40
41

42 **[insert Figure 4.]**
43
44

45 Fig.4. Ultimate tensile strength and Elongation of Cellulose acetate and TiO₂
46 films with different Ag content.
47
48
49

50 The general behaviour of Young's modulus was found to be depended on the
51 elongation and ultimate strength according to the filler contents and the
52 homogeneity of particle distribution within the CA matrix.
53
54
55
56

57 **[insert Figure 5.]**
58
59
60

1
2
3 Fig.5. Young modulus of Cellulose acetate and TiO₂ films with different Ag
4 content.
5
6
7

8 **4.3 FTIR spectroscopy**

9
10
11 Figures 6 show the FTIR spectra of pure CA film and CA films containing
12 different weight ratios of Ag nanoparticle (1.5, 2, 2.5) wt% and a constant
13 weight ratio of 2 wt%TiO₂. The film spectrum is characterized by the
14 presence of bands at 1741 cm⁻¹ (steric carbonyl stretching), 3478 cm⁻¹
15 (cellulose OH stretching), and 2936 cm⁻¹ (CH stretching) [31]. The bands of
16 2936 cm⁻¹ (CH stretching), 3478 cm⁻¹ (OH stretching), 1741 cm⁻¹ (steric
17 carbonyl stretching), 1232 cm⁻¹, and 1045 cm⁻¹ (C-O stretching), all
18 increased when Ag-TiO₂ nanoparticle were added. Because TiO₂ is an oxide
19 with O-Ti-O bonding in its chemical structure, inserting it into cellulose
20 acetate may have increased the interactions between the two compounds at
21 the region of the band that represented these properties. TiO₂ bonding is
22 represented by peaks at 600 cm⁻¹ and 750 cm⁻¹ [32,33]. Carbonian and
23 hydroxyl groups have peaks cantered at 1750 cm⁻¹ and 3478 cm⁻¹,
24 respectively [32]. The vibration frequency of Ag-O ionic bond groups is
25 indicated by the peak at 513 cm⁻¹. [34].
26
27
28
29
30
31
32
33
34
35
36
37
38
39
40
41
42

43 **[insert Figure 6.]**

44
45 Fig.6. FTIR spectra of Ag/TiO₂ based Cellulose acetate.

46 **4.4 Water contact angle**

47
48 The wettability test determines how many water molecules the sample
49 absorbs. The wettability character of the surface is broadly defined as
50 whether the sample is hydrophilic or hydrophobic. Water contact angles for
51 CA and Ag-TiO₂ /CA at different weight ratios of Ag nanoparticle (1.5, 2,
52 2.5) wt% and a constant weight ratio of 2 wt%TiO₂ are represented in Fig. 7.
53
54
55
56
57
58
59
60

1
2
3 Because of its hydrophilic nature, the CA film had the lowest surface
4 wettability of all the produced films, with a contact angle of 61.3° , as the
5 low surface wettability leads to a high contact angle, and vice versa [35]. All
6 composite films showed higher contact angles of 70.2, 72.4, and 76.4°
7 compared to CA film. The contact angle of the prepared films increased
8 towards hydrophobicity with an increase in nano Ag content in them [36].
9
10
11
12
13
14

15
16
17 **[insert Figure 7.]**
18

19 Fig.7. water contact angle for CA film and nanocomposite thick films with
20 various Ag content.
21
22

23 24 25 **4.5 Antibacterial activity** 26

27
28 The optical density of Escherichia coli and Staphylococcus aureus
29 suspensions at 600 nm treated with different films in test tubes for 12 hours
30 was measured, which is a commonly used method for determining the
31 growth of bacteria for the assessment of antibacterial activities [37,38]. In
32 general, the lower the optical density of bacteria suspension at 600 nm after
33 a specific period of cultivation, the better the antibacterial film's activity. As
34 shown in Fig. 8, the OD600 values for various antibacterial films were in the
35 following order: control > CA > CA/2%TiO₂/1.5%Ag > CA/2%TiO₂/2%Ag >
36 CA/2%TiO₂/2.5%Ag . It's important to note that the nanocomposite film
37 made up of CA+2% TiO₂+2.5% Ag had the lowest OD600. In contrast to
38 other antibacterial films, this film performed particularly well after 12 hours
39 of cultivation. These results clearly show that TiO₂ and Ag have a greater
40 ability to resist bacteria growth [39-44].
41
42
43
44
45
46
47
48
49
50
51
52
53
54

55
56 **[insert Figure 8.]**
57

58 Fig.8. Effect of CA and CA/TiO₂/Ag in *E. coli* and *S. aureus* growth
59 curve.
60

4. Conclusion

The present study used casting method to prepare Ag-TiO₂/ CA composite films. The tensile test proved that ultimate tensile strength and elongation were improved at fixed level of 1.5%Ag-2%TiO₂/CA, beyond that level of loading the values of tensile strength and elongation decreased. FTIR spectra demonstrated the interaction between CA and Ag-TiO₂. An increase towards hydrophobicity was also observed by the addition of Ag content. CA/TiO₂/Ag has enhanced antibacterial activity against Escherichia coli and Staphylococcus aureus compared with Pure CA. Due to the wettability properties and antibacterial activity of the prepared films, they could be used in packaging applications.

Reference

- [1] Lal S, Kumar V, Arora S. Eco-friendly synthesis of biodegradable and high strength ternary blend films of PVA/starch/pectin: Mechanical, thermal and biodegradation studies. *Polym and Polym Compos.* 2020 Nov 20;29(9):1505–14.
- [2] Arfat YA, Ejaz M, Jacob H, Ahmed J. Deciphering the potential of guar gum/Ag-Cu nanocomposite films as an active food packaging material. *Carbohydr Polym.* 2017 Feb;157:65–71.
- [3] Wang Z, Narciso J, Biotteau A, Plotto A, Baldwin E, Bai J. Improving Storability of Fresh Strawberries with Controlled Release Chlorine Dioxide in Perforated Clamshell Packaging. *Food Bioprocess Technol.* 2014;7(12):3516–24.
- [4] Giosafatto CVL, Di Pierro P, Gunning AP, MacKie A, Porta R, Mariniello L. Trehalose-containing hydrocolloid edible films prepared in the presence of transglutaminase. *Biopolymers.* 2014;101(9):931–7.

- 1
2
3 [5] Feng Z, Wu G, Liu C, Li D, Jiang B, Zhang X. Edible coating based on
4 whey protein isolate nanofibrils for antioxidation and inhibition of product
5 browning. Vol. 79, Food Hydrocolloids. 2018. p. 179–88.
6
7
8
9 [6] Sharma A, Giri SK, Kartha KPR, Sangwan RS. Value-additive
10 utilization of agro-biomass: preparation of cellulose triacetate directly from
11 rice straw as well as other cellulosic materials. RSC Adv.
12 2017;7(21):12745–52.
13
14
15 [7] Candido RG, Godoy GG, Gonçalves A. Characterization and application
16 of cellulose acetate synthesized from sugarcane bagasse. Carbohydr Polym.
17 2017;167:280–9.
18
19
20 [8] Samios E, Dart RK, Dawkins J V. Preparation, characterization and
21 biodegradation studies on cellulose acetates with varying degrees of
22 substitution. Vol. 38, Polymer. 1997. p. 3045–54.
23
24
25 [9] Holkem AT, Raddatz GC, Nunes GL, Cichoski AJ, Jacob-Lopes E,
26 Ferreira Grosso CR, et al. Development and characterization of alginate
27 microcapsules containing Bifidobacterium BB-12 produced by
28 emulsification/internal gelation followed by freeze drying. Vol. 71, LWT -
29 Food Science and Technology. 2016. p. 302–8.
30
31
32 [10] Li J, He J, Huang Y, Li D, Chen X. Improving surface and mechanical
33 properties of alginate films by using ethanol as a co-solvent during external
34 gelation. Vol. 123, Carbohydrate Polymers. 2015. p. 208–16.
35
36
37 [11] Sarkar S, Chakraborty S, Bhattacharjee C. Photocatalytic degradation
38 of pharmaceutical wastes by alginate supported TiO₂ nanoparticles in
39 packed bed photo reactor (PBPR). Vol. 121, Ecotoxicology and
40 Environmental Safety. 2015. p. 263–70.
41
42
43 [12] Wang H-MD, Chen C-C, Huynh P, Chang J-S. Exploring the potential
44 of using algae in cosmetics. Bioresour Technol. 2015 May;184:355–62.
45
46
47
48
49
50
51
52
53
54
55
56
57
58
59
60

- 1
2
3 [13] Chen H, Seiber JN, Hotze M. ACS select on nanotechnology in food
4 and agriculture: A perspective on implications and applications. Vol. 62,
5 Journal of Agricultural and Food Chemistry. 2014. p. 1209–12.
6
7
8
9 [14] Fasciani C, Silvero MJ, Anghel MA, Argüello GA, Becerra MC,
10 Scaiano JC. Aspartame-stabilized gold-silver bimetallic biocompatible
11 nanostructures with plasmonic photothermal properties, antibacterial
12 activity, and long-term stability. *J Am Chem Soc.* 2014;136(50):17394–7.
13
14
15 [15] Sturaro A, Rella R, Parvoli G, Ferrara D, Tisato F. Contamination of
16 dry foods with trimethyldiphenylmethanes by migration from recycled paper
17 and board packaging. *Food Addit Contam.* 2006;23(4):431–6.
18
19
20 [16] Goudarzi V, Shahabi-Ghahfarrokhi I. Photo-producible and photo-
21 degradable starch/TiO₂ bionanocomposite as a food packaging material:
22 Development and characterization. Vol. 106, *International Journal of*
23 *Biological Macromolecules.* 2018. p. 661–9.
24
25
26 [17] Youssef AM, El-Sayed SM, Salama HH, El-Sayed HS, Dufresne A.
27 Evaluation of bionanocomposites as packaging material on properties of soft
28 white cheese during storage period. Vol. 132, *Carbohydrate Polymers.* 2015.
29 p. 274–85.
30
31
32 [18] Tang S, Wang Z, Li P, Li W, Li C, Wang Y, et al. Degradable and
33 photocatalytic antibacterial Au-TiO₂/sodium alginate nanocomposite films
34 for active food packaging. *Nanomaterials.* 2018;8(11).
35
36
37 [19] Zhang D, Wen M, Zhang S, Liu P, Zhu W, Li G, et al. Au nanoparticles
38 enhanced rutile TiO₂ nanorod bundles with high visible-light photocatalytic
39 performance for NO oxidation. Vol. 147, *Applied Catalysis B:*
40 *Environmental.* 2014. p. 610–6.
41
42
43 [20] Clavero C. Plasmon-induced hot-electron generation at
44 nanoparticle/metal-oxide interfaces for photovoltaic and photocatalytic
45 devices. *Nat Photonics.* 2014;8(2):95–103.
46
47
48
49
50
51
52
53
54
55
56
57
58
59
60

- 1
2
3
4 [21] Liu E, Fan J, Hu X, Hu Y, Li H, Tang C, et al. A facile strategy to
5 fabricate plasmonic Au/TiO₂ nano-grass films with overlapping visible light-
6 harvesting structures for H₂ production from water. *J Mater Sci.*
7 2015;50(5):2298–305.
8
9
10
11 [22] Altomare M, Marelli M, Scotti R, et al. V. Pt and Au/TiO₂
12 photocatalysts for methanol reforming: Role of metal nanoparticles in tuning
13 charge trapping properties and photoefficiency. Vol.130, *Applied Catalysis*
14 *B: Environmental.* 2013. p. 239–248.
15
16
17 [23] Wang Y-G, Yoon Y, Glezakou V-A, Li J, Rousseau R. The role of
18 reducible oxide-metal cluster charge transfer in catalytic processes: new
19 insights on the catalytic mechanism of CO oxidation on Au/TiO₂ from ab
20 initio molecular dynamics. *J Am Chem Soc.* 2013 Jul;135(29):10673–83.
21
22
23 [24] Scuderi V, Impellizzeri G, Romano L, Scuderi M, Bergum K, Zimbone
24 M, et al. An enhanced photocatalytic response of nanometric TiO₂ wrapping
25 of Au nanoparticles for eco-friendly water applications. vol 6, *Nanoscale*
26 .2014, 6, p.11189–11195.
27
28 [25] Hayajneh MT, Al-Oqla FM, Al-Shrida MM. Hybrid green
29 organic/inorganic filler polypropylene composites: Morphological study and
30 mechanical performance investigations. *E-Polymers.* 2021;21(1):710–21.
31
32 [26] Zare Y, Rhee KY. Analysis of critical interfacial shear strength between
33 polymer matrix and carbon nanotubes and its impact on the tensile strength
34 of nanocomposites. Vol. 9, *Journal of Materials Research and Technology.*
35 2020. p. 4123–32.
36
37 [27] Hamad QA, Oleiwi JK, Abdulrahman SA. Tensile properties of
38 laminated composite prosthetic socket reinforced by different fibers.
39 *Materials Today: Proceedings.* 2021.
40
41 [28] Ndukwe CO, Ezurike BO, Okpala PC. Comparative studies of
42 experimental and numerical evaluation of tensile properties of Glass Fibre
43 Reinforced Polyester (GFRP) matrix. *Heliyon.* 2021;7(5):e06887.
44
45
46
47
48
49
50
51
52
53
54
55
56
57
58
59
60

- 1
2
3 [29] Noguchi T, Endo M, Niihara K, Jinnai H. Cellulose nanofiber/elastomer
4 composites with high tensile strength, modulus, toughness, and thermal
5 stability prepared by high-shear kneading. vol. 188. *Composites Science and*
6 *Technology*. 2020. p.108005.
7
8
9
10
11 [30] P D, Narayanankutty SK. Styrenated phenol modified nanosilica for
12 improved thermo-oxidative and mechanical properties of natural rubber.
13 Vol. 82, *Polymer Testing*. 2020.
14
15
16
17 [31] Gonçalves SM, dos Santos DC, Motta JFG, Santos RR dos, Chávez
18 DWH, Melo NR de. Structure and functional properties of cellulose acetate
19 films incorporated with glycerol. Vol. 209, *Carbohydrate Polymers*. 2019. p.
20 190–7.
21
22
23
24
25 [32] Naghibi S, Gharagozlou M, Vahed S. Antibacterial response of Cd-
26 TiO₂/PEG/folic acid nanocomposite under ultraviolet, visible light, or
27 ultrasonic irradiation. *J Nanostructures*. 2019;9(4):768–75.
28
29
30
31 [33] Mehdizadeh P, Tavangar Z. Photocatalyst Ag@N/TiO₂ nanoparticles:
32 Fabrication, characterization, and investigation of the effect of coating on
33 methyl orange dye degradation. *J Nanostructures*. 2017;7(3):216–22.
34
35
36
37 [34] Gharibshahi L, Saion E, Gharibshahi E, Shaari AH, Matori
38 KA. Structural and Optical Properties of Ag Nanoparticles Synthesized by
39 Thermal Treatment Method. Vol 10. *nanomaterial journal*. 2017. p.402.
40
41
42
43 [35] Al-Naamani L, Dobretsov S, Dutta J. Chitosan-zinc oxide nanoparticle
44 composite coating for active food packaging applications. Vol. 38,
45 *Innovative Food Science and Emerging Technologies*. 2016. p. 231–7.
46
47
48
49 [36] Baig N, Kammakam I. Removal of Oily Contaminants from Water
50 by Using the Hydrophobic Ag Nanoparticles Incorporated Dopamine
51 Modified Cellulose Foam. Vol 13. *Polymers journal*. 2021. p.3163.
52
53
54
55 [37] Bahjat H, Ismail R, Sulaiman G, Jabir M. Magnetic Field-Assisted
56 Laser Ablation of Titanium Dioxide Nanoparticles in Water for Anti-
57 Bacterial Applications. *J Inorg Organomet Polym Mater*. 2021 Sep 1;31.
58
59
60

1
2
3 [38] Jihad MA, Noori FTM, Jabir MS, Albukhaty S, Almalki FA, Alyamani
4 AA. Polyethylene glycol functionalized graphene oxide nanoparticles loaded
5 with nigella sativa extract: A smart antibacterial therapeutic drug delivery
6 system. *Molecules*. 2021;26(11).
7

8
9
10
11 [39] Albukhaty S, Albayati L, Alkaragoly H, Al-Musawi S. Preparation and
12 characterization of titanium dioxide nanoparticles and in vitro investigation
13 of their cytotoxicity and antibacterial activity against *Staphylococcus aureus*
14 and *Escherichia coli*. *Anim Biotechnol*. 2020 Nov 28.
15

16
17 [40] Albukhaty S, Alkaragoly H, Dragh M. Synthesis of zinc oxide
18 nanoparticles and evaluated its activity against bacterial isolates. *J Biotech*
19 *Res*. 2020 Jan 11;11:47–53.
20

21
22 [41] Jabir MS, Hussien AA, Sulaiman GM, Yaseen NY, Dewir YH,
23 Alwahibi MS, et al. Green synthesis of silver nanoparticles from *Eriobotrya*
24 *japonica* extract: a promising approach against cancer cells proliferation,
25 inflammation, allergic disorders and phagocytosis induction. *Artif Cells,*
26 *Nanomedicine, Biotechnol*. 2021 Jan 1;49(1):48–60.
27

28
29 [42] Jabbar R, Hussein N. Evaluation The Antibacterial Activity of
30 Biosynthesis Silver Nanoparticles by *Lactobacillus Gasseri* Bacteria. *J Appl*
31 *Sci Nanotechnol*. 2021;1(3):86–95.
32

33
34 [43] Hussein N, Khadum MM. Evaluation of the Biosynthesized Silver
35 Nanoparticles’ Effects on Biofilm Formation. *J Appl Sci Nanotechnol*.
36 2021;1(1):23–31.
37

38
39 [44] AL-Ogaili AK , Ali AK , Ali TH. Preparation of Silver Nanoparticles
40 and Study the Optical and Antibacterial Properties. Vol 33.
41 *Eng&Tech.Journal*.2015.p.478–87.
42
43
44
45
46
47
48
49
50
51
52
53
54
55
56
57
58
59
60

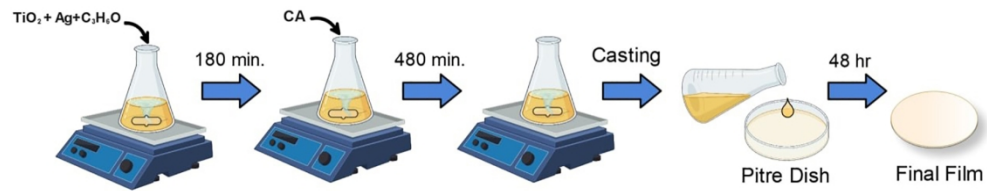


Fig. 1. Schematic diagram of the preparation process for the films.

162x33mm (300 x 300 DPI)

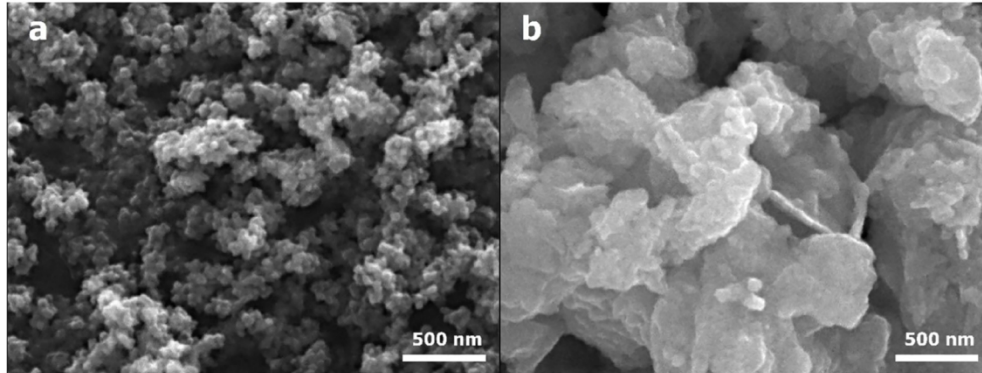


Fig.2. SEM images of (a) TiO₂ nanoparticle, (b) Ag nanoparticle.

150x58mm (300 x 300 DPI)

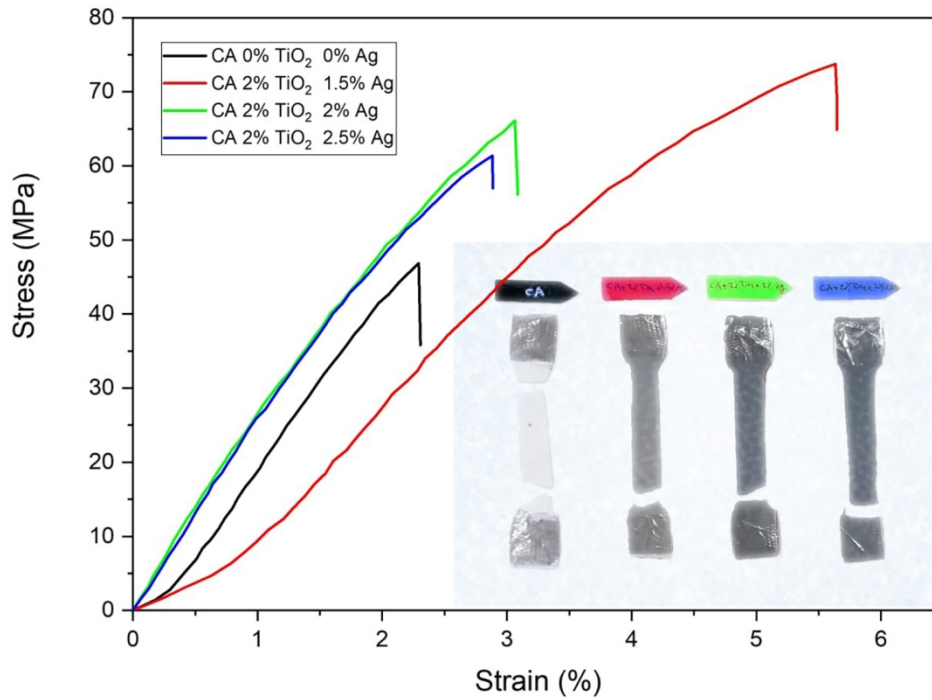


Fig.3. stress-strain curve of Ag/TiO₂ with Cellulose acetate.

135x103mm (300 x 300 DPI)

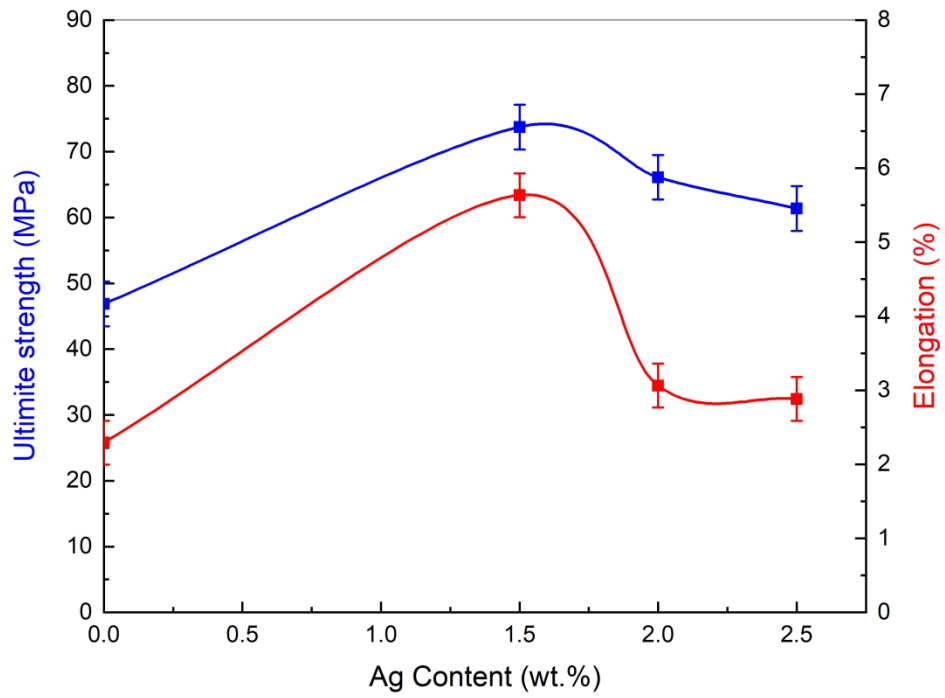


Fig.4. Ultimate tensile strength and Elongation of Cellulose acetate and TiO₂ films with different Ag content.

272x208mm (300 x 300 DPI)

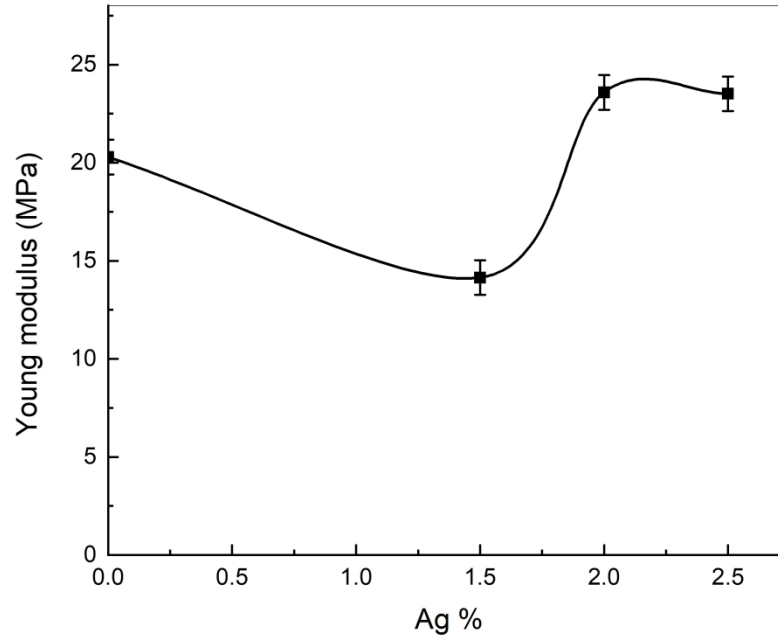


Fig.5. Young modulus of Cellulose acetate and TiO₂ films with different Ag content.

272x208mm (300 x 300 DPI)

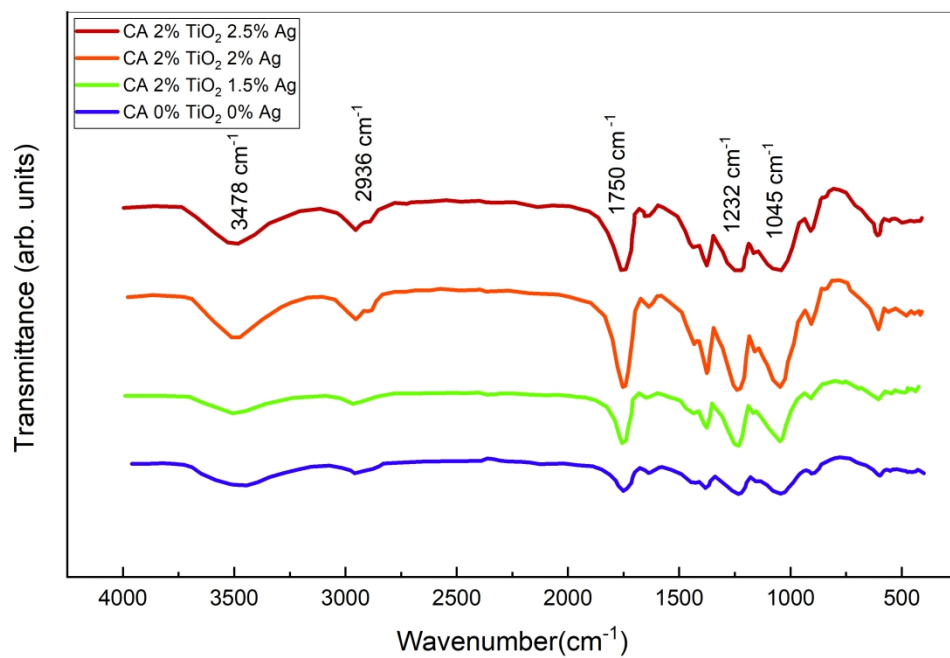


Fig.6. FTIR spectra of Ag/TiO₂ based Cellulose acetate.

287x201mm (300 x 300 DPI)

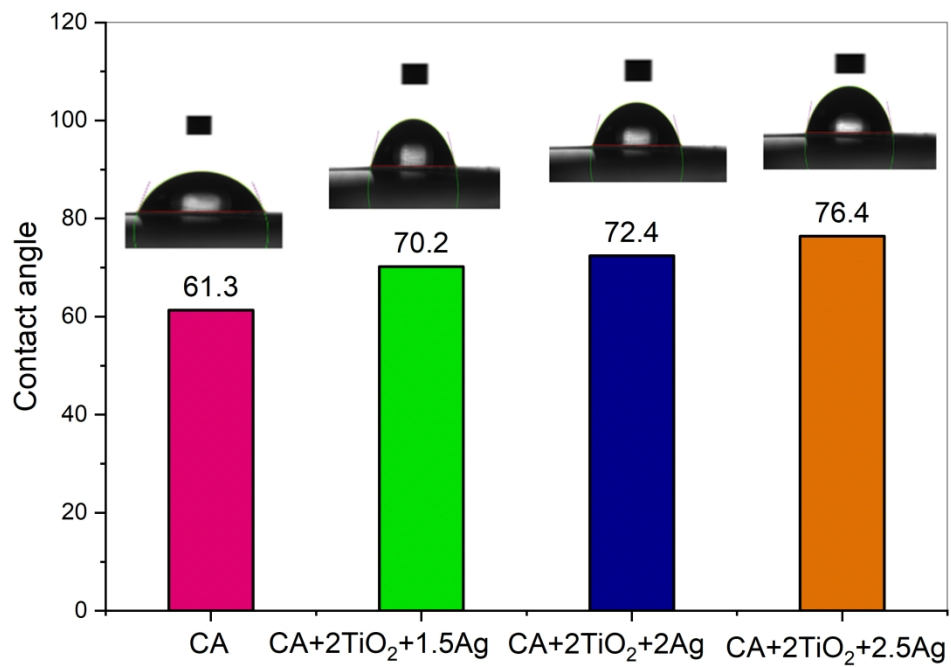


Fig.7. water contact angle for CA film and nanocomposite thick films with various Ag content.

272x208mm (300 x 300 DPI)

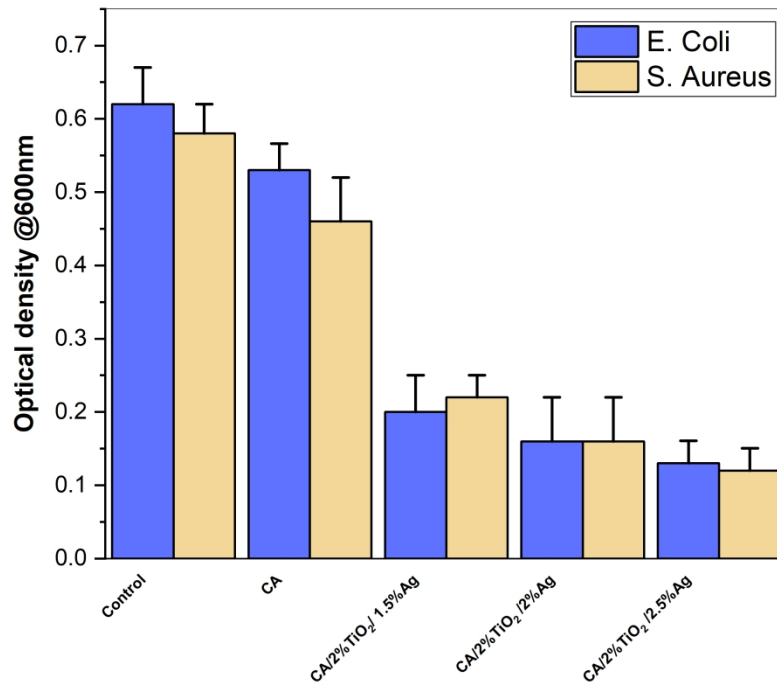


Fig.8. Effect of CA and CA/TiO₂/Ag in E. coli and S. aureus growth curve.

272x208mm (300 x 300 DPI)